Journal of Cleaner Production 232 (2019) 1121–1133

Contents lists available at ScienceDirect

Journal of Cleaner Production

journal homepage: www.elsevier.com/locate/jclepro

An optimization model for energy-efficient machining for sustainable production

Honghui Wang [a, b], Ray Y. Zhong [c], Guijie Liu [a, b, *], WeiLei Mu [a, b], Xiaojie Tian [a, b], Dingxin Leng [a, b]

[a] Department of Mechanical and Electrical Engineering, Ocean University of China, Qingdao, 266100, China
[b] Key Laboratory of Ocean Engineering of Shangdong Province, Ocean University of China, Qingdao, 266100, China
[c] Department of Industrial and Manufacturing Systems Engineering, The University of Hong Kong, Hong Kong

ARTICLE INFO

Article history:
Received 9 July 2018
Received in revised form
20 May 2019
Accepted 24 May 2019
Available online 30 May 2019

Keywords:
STEP-NC
Ant colony optimization algorithm
Energy-efficient machining

ABSTRACT

Sustainable production plays an important role in product lifecycle management by considering the social sustainability. Energy-efficient machining is an efficient approach for sustainable production in current manufacturing sectors. Although many related efforts have been achieved, a comprehensive energy optimization approach oriented to manufacturing parts is still a challenge. Therefore, this paper selects Standard for the Exchange of Product model data-Numerical Control (STEP-NC) as the enabling technology to achieve energy-efficient machining. An optimization model is proposed based on the energy calculation method using the workingstep in STEP-NC. An improved ant colony optimization (ACO) solution, consisting of encoding and decoding, initialization, machining scheme generation, idea of local multiple iteration, evaluation, pheromone evaporation and update, is presented. A part with typical manufacturing features is applied to verify the effectiveness of the proposed approach. The generated solution can provide a comprehensive machining scheme for low energy demandI by improving the efficiency with 25% for solving the optimization problem.

1. Introduction

Due to soaring energy prices and environmental pollution, research on sustainable product lifecycle management (SPLM) has been focused recently. Sustainable production is one important phase of SPLM. Reducing energy consumption during machining operations plays a critical role in achieving sustainable production, i.e., energy-efficient machining. Energy-efficient machining has attracted increasingly more efforts in recent years (Camposeco-Negrete, 2013; Gong et al., 2016; Velchev et al., 2014; Yan and Li, 2013; Zhou et al., 2016).

Deciding machining schemes (MSs) for a part to be machined from the perspective of energy efficiency is an effective way to perform energy-efficient machining. A MS consists of many key elements, e.g., machining resources, machining parameters, tool path, process route, etc. In general, there exist more than one reasonable MS, which could constitute a group of candidate machining schemes (CMSs), and the best machining scheme (BMS), i.e., energy-efficient machining scheme (EEMS), is generated from this group. It is obvious that this process refers to an optimization problem. To solve the optimization problem, two key procedures are necessary, i.e., optimization model and the corresponding solution method. An optimization model includes optimization objective, optimization variables and constraints. The objective may be single (i.e. only energy consumption) or multiple (e.g. time, energy, tool life, etc.). No matter single-objective or multiple-objectives optimization, an energy consumption model for indicating the energy calculation approach during machining processes is essential, which is used to formulating the optimization objective. Besides, the optimization variables are the contributing factors to the objective, and the constraints are determined in terms of the specific conditions. Regarding the solution method, a meta-heuristic algorithm is a type of effective method of solving the optimization model, such as genetic algorithm (GA), ant colony optimization (ACO), particle swarm optimization (PSO), tabu search (TS), simulated annealing (SA) and NSGA-II. Nowadays, many kinds of optimization models have been built with related solution methods, which promoted the development of energy-efficient

* Corresponding author. Department of Mechanical and Electrical Engineering, Ocean University of China, Qingdao, 266100, China.
E-mail address: liuguijie@ouc.edu.cnm (G. Liu).

https://doi.org/10.1016/j.jclepro.2019.05.271
0959-6526/© 2019 Elsevier Ltd. All rights reserved.

machining. However, the established optimization models mainly concern on a certain factor or portions of factors to energy consumption in a MS, so that the energy cannot be optimized from a holistic perspective during production processes. This paper adopts Exchange of Product model data-Numerical Control (STEP-NC) (ISO14649-1, 2003) as the key enabling technology to achieve energy-efficient machining for sustainable production, where an optimization model for energy-efficient machining is built and its solution method with an improved ACO is presented. The core concept of STEP-NC, i.e., workingstep, is applied to the base for calculating energy consumption for a part, where a finite state machine model is proposed to illustrate the execution process of workingstep. Accordingly, an optimization model is established in terms of the calculation method of energy consumption and the constraints, where workingstep and the sequence are considered jointly. An improved ACO is chosen to solve the optimization model, and the key procedures (i.e., encoding and decoding, initialization, machining scheme generation, evaluation, idea of local multiple iteration, pheromone evaporation and update) are given.

The rest of this paper is organized as follows. Section 2 gives the literature review about energy consumption calculation methods and energy optimization. Section 3 presents a brief introduction of STEP-NC approach used in this work. The energy consumption calculation method via STEP-NC is shown in Section 4. Section 5 builds optimization model by considering energy consumption. The model solutions with an improved ACO are illustrated in Section 6. Section 7 gives a case study where the proposed model is examined. Detailed discussions are given in this section too. Section 8 concludes this paper by giving our contributions and future work.

2. Literature review

2.1. Energy consumption calculation methods

To establish the optimization model, an effective calculation method of energy consumption is necessary. A machine tool is the basic energy unit during manufacturing process, therefore, the energy characteristic of a machine tool is the key to achieve energy consumption calculation for a part. Lv et al. (2016) investigated CNC machine tools energy characteristics by experimental studies, where the power consumption formulations of main components of a machine (e.g., spindle, feed axis) were displayed. Besides, Zhong et al. (2016) reviewed the power calculation approaches to cutting processes, and gave the corresponding accuracy of each method. Based on the above literature, some energy models were established from diverse perspectives. For example, Avram and Xirouchakis (2011) proposed an energy demand model for calculating the total energy required by a machine tool system for milling processes. Jia et al. (2014, 2016) introduced Therblig to represent the basic energy consumption unit, and the energy demand was obtained by linking the activities of machining processes and Therblig. Aramcharoen and Mativenga (2014) studied the energy intensity in machining processes and then built an energy consumption model by identifying key energy states. Lv et al. (2018) studied the turning energy consumption calculation approaches through investigating three power prediction methods. This effort could improve the accuracy of predicting the material removal power in turning processes. Shi et al. (2018) established a novel energy consumption model for milling process considering tool wear progression with experimental method, where this model not only achieved the energy consumption calculation but also predicted the tool wear. Yoon et al. (2018) investigated power characteristics of a rotational axis of a machine tool to build the corresponding empirical energy consumption model. Altıntaş et al. (2016) presented an energy consumption prediction model based on STEP224, which can run with 5% accuracy for the estimation of the theoretical energy demand during milling processes. Borgia et al. (2017) proposed an energy prediction method using simulation approach for milling operations, where power consumption of spindle, axes, and auxiliary units were considered. In addition, some researchers adopted specific energy consumption (SEC) to model the problem. For example, Liu et al. (2015) empirically analysed the relationship between the total power consumed by the machine tool and the cutting power at the tool tip, and accordingly the SEC model was obtained. Kara and Li (2011) adopted SEC to present an empirical model that characterized the relationship between energy consumption and process variables for material removal processes.

2.2. Energy consumption optimization

The optimization model is established according to the diverse energy consumption calculation methods, which in general is used to formulating the optimization objective with energy. The energy optimization can be performed through optimizing parameters, process route, job shop scheduling, etc. Some studies have achieved energy-efficient machining by optimizing parameters. Deng et al. (2017) minimized the energy consumption based on cutting SEC. In this work, a multi-objective optimization model aiming at SEC and time was built and transformed into a single objective with weights method, and the quantum genetic algorithm was used to solve this optimization problem. Li et al. (2019) presented a multi-objective parameter optimization method for energy efficiency in CNC milling processes, where the energy model of CNC milling was then established and it was solved by TS algorithm. Yi et al. (2015) built an optimization model to minimize carbon emissions during machining processes, and NSGA-II was adopted to solve the problem. Chen et al. (2015) analysed the energy consumption of multi-pass CNC milling, and then a multi-objective optimization model was proposed to maximize the energy efficiency and minimize the production cost. In this work, the optimization problem was solved by PSO. Li et al. (2014) introduced a multi-objective optimization model to achieve low energy consumption and high production rate simultaneously, and GA was used to solve it. In (Wang et al., 2014), energy consumption, cost and quality were considered to establish the optimization model, and NSGA-II was used to resolve the problem. Ma et al. (2017) proposed an energy saving strategy for milling processes, where the impacts of cutting parameters on energy were fully considered and matlab toolbox was directly used to achieve the optimization. Apart from parameter optimization, process route selection is also an effective approach to reducing energy consumption. Tan (2004) built an optimization model oriented to process routes for green manufacturing, and this model was solved by SA. A typical part was used to verify the effectiveness of the proposed method. Some studies addressed job shop scheduling to decrease energy demand. Gong et al. (2016) presented a generic method for energy-efficient and energy-cost-effective production at the unit process level. In this research, a mixed-integer linear programming mathematical model was formulated for energy-cost-aware job order scheduling on a single machine, and GA was implemented to search for an energy-cost-effective schedule. Zhang et al. (2016) minimized the machining system energy through integration of process planning and scheduling, where the integrated energy saving model was built and a GA-based approach was adopted to solve the established model. He et al. (2015) also used a mixed-integer linear programming method to establish an optimization model, including machine tool selection and operation sequence for scheduling. Nested partitions algorithm was adopted to solve the problem. Shrouf et al. (2014)

targeted single machining sustainable scheduling to formulate an energy consumption optimization model, which was solved by GA.

3. STEP-NC enabled approach

STEP-NC (i.e. ISO14649) is a series of standards for remedying the shortcomings of ISO6983 by specifying a machining process rather than a machine tool motion. It consists of a group of data structures (as shown in Fig. 1) built with EXPRESS language to describe sufficient high-level contents for a part to be manufactured (e.g. geometries, machining processes, and machining resources). Thus Peng and Xu (2017) regard it as a smart enabling technology to link up main components of product lifecycle management (e.g. design and manufacturing). With the support of the information through STEP-NC, energy evaluation and optimization for a part can be performed. The main characteristic of STEP-NC is feature-based and workingstep-oriented: the features are applied to represent the material to be removed in a part, and the workingstep is employed to describe the process information, e.g., the machining parameters. Besides, STEP-NC provides some candidate machining operations (e.g., plane rough milling (PRM), plane finish milling (PFM), etc.) and strategies (e.g., bidirectional (BD), unidirectional (UD), contour parallel (CP), etc.). In the context of STEP-NC, a STEP-NC Part 21 file is used to instantiate these data structures to constitute a MS for a part to be manufactured. To determine a MS compliant with STEP-NC considering energy efficiency is the research purpose in this work.

Fig. 2 gives the workflow of energy-efficient machining using STEP-NC approach. In the whole process, STEP-NC is the core concept to integrating each procedure: features are used to represent the part; with our previous work (Wang et al., 2018), CMSs for this part can be generated as the solution space of the optimization model; there are some contributing factors to energy consumption in a MS with STEP-NC, and these factors are the variables to calculating the energy of the part; the workingstep is selected as the key to organize these variables for energy consumption calculation; with this calculation method, the optimization model can be built; ACO is improved in terms of STEP-NC data structure to make itself more suitable to solve this model. Finally, the EEMS is determined. The details are presented in the following sections.

4. Energy consumption calculation via STEP-NC

4.1. Calculation method of energy consumption

Workingstep is defined as the basic unit to calculate the energy consumption. The energy demand of machining a part is the sum of each workingstep energy consumption, which is shown in Eq. (1).

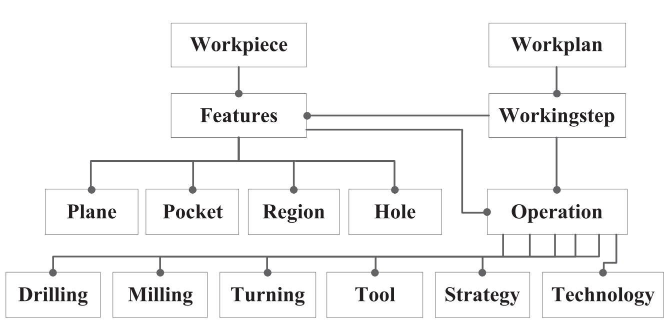

Fig. 1. Data structure of STEP-NC.

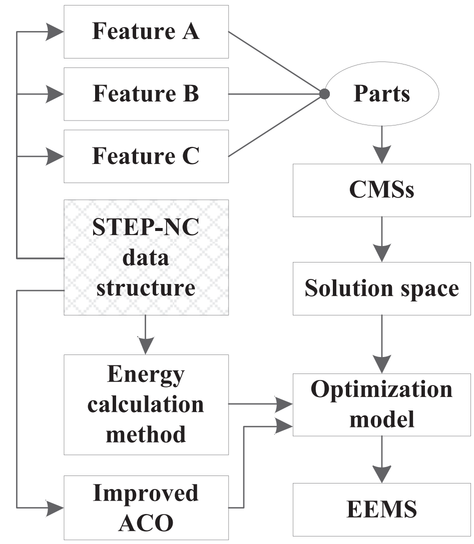

Fig. 2. Energy-efficient machining using STEP-NC approach.

$$E_{part} = \sum_{i=1}^{n} E_{ws,i} \tag{1}$$

where E_{part} represents the energy consumption of machining a part [J], $E_{ws,i}$ is the ith workingstep energy [J], and n is the count of workingsteps.

Eq. (1) is preliminary for calculation of a part's energy consumption. To achieve energy demand calculation, the finite state machine of a workingstep is established, as shown in Fig. 3.

According to Fig. 3, the states of a workingstep and the transition condition of each state are presented with the execution process of a workingstep. The value of E_{ws} can be obtained by the sum of each state's energy consumption, as shown in Eq. (2).

$$E_{ws} = E_p + E_a + E_l + E_m \tag{2}$$

where E_p represents the energy demand of the preparation state [J], E_a is the energy demand of the approaching state [J], E_l is the energy demand of the leaving state [J], and E_m is the energy demand of the machining state [J].

Before specifying the approach to calculating the energy demand of the four states, the power-driven components of a machine tool are re-classified:

- The basic components (BC): They refer to the components that must run when a machine tool is on, e.g. the controller, monitor and fan.
- The machine tool function components (MTFC): They refer to the components that will run according to the corresponding conditions when a machine tool is on. They can be further divided into two types:
  - The workingstep-related components (WRC): They are the subtypes of machine tool function components, but the power of these components is related to workingstep, e.g. tool changer.
  - The workingstep-unrelated components (WURC): They are the subtypes of machine tool function components, but the power of these components is unrelated to workingstep, e.g. light and cutting fluid.
- The components for cutting: They refer to the spindle and feed axis in this paper.

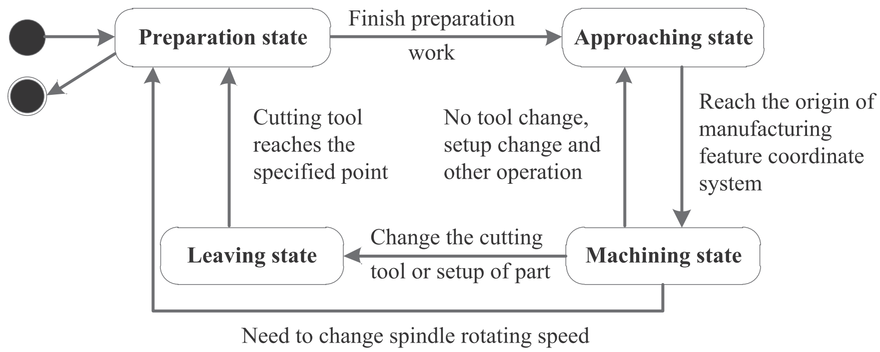

Fig. 3. Finite state machine of workingstep.

The BC, WURC and spindle remain running in entire machining processes. Excluding the spindle, the power of the BC and WURC are constant, Eq. (3) is used to calculate their energy consumption E_{b,ws_nr} [J].

$$E_{b,ws\_nr} = (P_{ws,nr} + P_b)t_{total} \tag{3}$$

where $P_{ws,nr}$ is the power of WURC [W], P_b is the power of BC [W], and t_{total} is the total time of machining a part [s], which meets Eq. (4).

$$t_{total} = \sum_{i=1}^{n}(t_{p,i} + t_{l,i} + t_{a,i} + t_{m,i}) \tag{4}$$

where $t_{p,i}$ refers to the preparation state time of the ith workingstep [s], $t_{l,i}$ is the leaving state time of the ith workingstep [s], $t_{a,i}$ is the approaching state time of the ith workingstep [s], and $t_{m,i}$ is the machining state time of the ith workingstep [s].

For the spindle, its power demand meets a linear model, and the variable is the spindle rotating speed (Lv et al., 2016). Because different workingsteps may use different spindle rotating speeds, the energy consumption should be considered as shown in Eq. (5)

$$E_{sp} = P_{sp}\left(t_l + t_a + t_m + t_p^{'}\right) \tag{5}$$

where E_{sp} is the spindle energy consumption of a workingstep [J], P_{sp} is the power of the spindle of a workingstep [W], t_l is the leaving state time of a workingstep [s], t_a is the approaching state time of a workingstep [s], t_m is the machining state time of a workingstep [s], and $t_p^{'}$ is the preparation state time of spindle preparation [s].

Based on the above discussion, Eq. (1) can be rewritten as Eq. (6).

$$E_{part} = E_{b,ws\_nr} + \sum_{i=1}^{n}\left(E_{sp,i} + E_{p,i}^{'} + E_{a,i}^{'} + E_{l,i}^{'} + E_{m,i}^{'}\right) \tag{6}$$

where $E_{sp,i}$ is the spindle energy consumption of the ith workingstep [J], $E_{p,i}^{'}$ is the updated preparation state energy consumption of the ith workingstep [J], $E_{a,i}^{'}$ is the updated approaching state energy consumption of the ith workingstep [J], $E_{l,i}^{'}$ is the updated leaving state energy consumption [J], and $E_{m,i}^{'}$ is the updated machining state energy consumption of the ith workingstep [J].

4.1.1. Preparation state

The preparation state mainly includes the energy consumption of workingstep-related components, changing the spindle rotating speed, spindle starting and spindle stopping, which can be represented by Eq. (7).

$$E_p^{'} = E_{ws\_r} + E_{sp\_s} + E_{sp\_on} + E_{sp\_off} \tag{7}$$

where E_{ws_r} is the energy consumption of workingstep-related components [J], E_{sp_s} is the energy consumption of changing the spindle rotating speed [J], E_{sp_on} is the energy consumption of spindle starting [J], and E_{sp_off} is the energy consumption of spindle stopping [J].

The energy consumption of E_{sp_s}, E_{sp_on}, E_{ws_r} and E_{sp_off} can be approximately represented by a constant value. This paper uses the average value of the corresponding process to express the energy consumption.

4.1.2. Approaching and leaving state

Regarding the approaching state and leaving state, the motions of these two are rapid traverse of the feed axis. The power of the feed axis meets a linear model or a square model. The feed velocity is the variable and the other coefficients are fixed. During rapid traverse, the power of feed axis is a constant, which could be presented by Eq. (8).

$$E_{a,l} = P_{a,l}t_{a,l} = \frac{P_{a,l}}{v_r}l_{a,l} = k_{a,l}l_{a,l} \tag{8}$$

where $E_{a,l}$ represents $E_a^{'}$ or $E_l^{'}$, $P_{a,l}$ is the power of the feed axis in the approaching state or leaving state [W], v_r is the velocity of rapid traverse [mm/min], $l_{a,l}$ is the distance of rapid traverse [mm], and $k_{a,l}$ is a coefficient that equals $P_{a,l}$ divided by v_r.

4.1.3. Machining state

The machining state performs the key function of a machine tool, i.e. removal of redundant materials. This state may involve three motion types in terms of machining strategies, and its energy consumption E_m meets Eq. (9).

$$E_m = E_{m\_r} + E_{m\_f} + E_{m\_c} \tag{9}$$

where E_{m_r} is the energy consumption of rapid traverse in the machining state [J], E_{m_f} is the feed axis energy consumption in the machining state [J], and E_{m_c} is the cutting energy consumption in the machining state [J].

E_{m_r} mainly depends on the distance of rapid traverse in the same machine tool (the calculation method refers to Eq. (8)), while E_{m_f} and E_{m_c} depend on not only the moving distance but also the machining parameters.

Similar to Eq. (8), E_{m_f} can be obtained by Eq. (10).

$$E_{m\_f} = P_{m\_f} t_{m\_f} = \frac{P_{m\_f}}{v_f} l_{m\_f} \tag{10}$$

where P_{m_f} is the feed axis power [W], t_{m_f} is the moving time [s] of the feed axis with feed velocity v_f [mm/min], and l_{m_f} is the motion distance [mm] of the feed axis with v_f.

For E_{m_c}, its calculation meets Eq. (11).

$$E_{m\_c} = P_{m\_c} t_{m\_c} = P_{m\_c} \frac{l_{m\_c}}{v_f} \tag{11}$$

where P_{m_c} is the cutting power [W], t_{m_c} is the cutting time [s], l_{m_c} is the motion distance of the feed axis [mm].

In this paper, a milling process and a drilling process are mainly considered. The power calculation method of the two processes can refer to Eq. (12) and Eq. (13) (Lv et al., 2016).

$$P_{m\_c} = P_M = C_M a_p^{x_M} f_z^{y_M} v_M^{n_M} a_w^{u_M} \tag{12}$$

where P_M is the milling power [W], C_M, x_M, y_M, n_M, and u_M are the coefficients, a_p is the axial cutting depth [mm], f_z is the feed per tooth [mm/z], v_M is the cutting velocity for milling [m/min], and a_w is the radial cutting depth [mm].

$$P_{m\_c} = P_D = C_D f_r^{y_D} v_D^{n_D} \tag{13}$$

where P_D is the drilling power [W], C_D, y_D and n_D are the coefficients, f_r is the feed per revolution [mm/r], and v_D is the cutting velocity for drilling [m/min].

In Eq. (10) and Eq. (11), the motion distance of the feed axis depends on machining parameters and strategies, which can be expressed by Eq. (14).

$$l_{m\_f},\ l_{m\_c} = \frac{l_s(t_s, a_p, a_w)}{v_f} \tag{14}$$

where t_s is the type of machining strategies and l_s [mm] is a function of t_s, a_p and a_w.

5. Proposed model by considering energy consumption

This section introduces the optimization model based on the calculated energy consumption.

5.1. Determination of optimization variables

In this research, optimization variables involve: (1) machine tool (*MT*); (2) cutting tool (*C*); (3) cutting parameters (*P*); (4) machining strategy (*S*); (5) material (*M*); and (6) sequencing of workingsteps. The above optimization variables will constitute a machining scheme (*MS*) that is compliant with STEP-NC.

5.2. Optimization objective

The energy-efficiency of machining a part is the optimization objective. In this work, *SEC* is used to represent the energy-efficiency, which is shown as Eq. (15).

$$SEC = \frac{E_{part}}{V_{part}} \tag{15}$$

where V_{part} is the volume of the part [mm^3].

5.3. Constraints

Because this work considers generation of workingstep and the sequencing, the set of constraints should be organized as follows.

For a workingstep, the basic constraints are shown as Eq. (16).

$$\begin{cases} p_{min} \le p \le p_{max} \\ F_{cut} \le F_{max} \\ P_{cut} \le P_{max} \end{cases} \tag{16}$$

where p are the machining parameters of a workingstep, F_{cut} is the cutting forcing during execution of a workingstep [N], and P_{cut} is the cutting power during executing a workingstep [W]. The above three variables should be within the corresponding ranges. p_{min} and p_{max} are the minimum and maximum of p, respectively. F_{max} and P_{max} are the maximum of F_{cut} and P_{cut} that a machine tool can support, respectively.

Some workingsteps should meet the roughness requirement. For milling processes, the roughness value after machining can be formulated as Eq. (17) (Wang et al., 2018).

$$R_a = \frac{f^2}{18\sqrt{3 r_t}} \le R_{max} \tag{17}$$

where R_a is the arithmetic surface roughness, r_t is the tool nose radius, and R_{max} is the maximum of the required R_a.

Parameters are the main factors to affecting the life of a cutting tool, and the mathematical relationship is shown as Eq. (18) (Shi et al., 2018).

$$T = \left(\frac{C_V k_V d^{q_V}}{v_c f_z^{y_V} a_p^{x_V} a_w^{u_V} z^{p_V}} \right)^{m^{-1}} \ge T_l \tag{18}$$

where T is the tool life [h], C_V, k_V, q_V, y_V, x_V, u_V, and p_V are the coefficients, and T_l is the expected tool life [h].

Some sequencing constraints of workingsteps should also be concerned, namely, the process principle (e.g., benchmark priority). This paper uses the following approach to formalizing constraints of sequencing.

i and j are used to represent the identity of workingstep. Function f_s can return the number of workingsteps in the sequencing with the input of the identity, where the result can be marked as S. Then, $S_i = f_s(i)$, and $S_i = f_s(i)$. It is assumed that workingstep i must be finished before workingstep j under some constraints, i.e. $S_i < S_j$. Therefore, Eq. (3) can be used to formalize the order of two workingsteps.

$$F_s = \begin{cases} 1, & S_i < S_j \\ 0, & else \end{cases} \tag{19}$$

where F_s is the discriminant function, and it can determine the satisfaction of the constraint. Furthermore, there are more than a pair of workingsteps that should be constrained. To solve it, continued multiplication is used, which is formalized as Eq. (20)

$$F = \prod_{i=1}^{n} \prod_{j=1}^{m} F_{s,i,j} \tag{20}$$

where F is the final discriminant function, and it can determine whether all constraints can be satisfied in a sequencing of workingsteps. $F_{s,i,j}$ represents the discriminant function of workingstep i and workingstep j.

From Eq. (20), the optimization process is reasonable under the premise of F equals to 1.

According to the above description, the optimization model can be established, which is shown as Eq. (21).

$$min\ \ SEC\ s.t.\ \ p_{min} \le p \le p_{max}\ \ F_{cut} \le F_{\,max}\ P_{cut} \le P_{\,max}\ T \ge T_l\ R_a = \frac{f^2}{18\sqrt{3r_t}} \le R_{max}\ F = 1 \tag{21}$$

6. An improved ACO solution for the proposed model

6.1. Encoding and decoding

The purpose of encoding is to represent each candidate machining scheme, while decoding is to transfer the encoded numbers to achieve the evaluation of energy consumption.

The objectives of encoding are optimal variables. In a workingstep, it involves MT, C, P, S and M. Except for P, other elements can use continuous natural numbers to achieve the encoding. Machining parameters can be further divided into sub-parameters, e.g. a_p in the milling processes. Each sub-parameter is generally a real number and has its own accuracy. Therefore, the encoding of each sub-parameter N_p is expressed as Eq. (22).

$$0 \le N_p \le \frac{p_{max} - p_{min}}{acc} \tag{22}$$

where p_{max} is the maximum of the sub-parameter, p_{min} is the minimum of the sub-parameter, and acc represents the accuracy (e.g. 0.1, 0.01).

The above description gives the approach to encoding, and the decoding method can be found in Eq. (23).

$$p_{max} = p_{min} + accN_p \tag{23}$$

The range of parameters depend on the combination of machine tool, cutting tool and material. Thus, it is necessary to describe the combination N_{com}, as follows:

$$N_{com} = N_c N_M i + N_M j + k,\ \ 0 \le i \le N_{MT}, 0 \le j \le N_c, 0 \le k \le N_M \tag{24}$$

where i, j and k are the encoded numbers of MT, C and M, respectively, and N_{MT}, N_c and N_M are the maximum encoded numbers of MT, C and M, respectively.

Each workingstep can also be represented by a natural number. A reasonable workingstep sequence can be abstracted as a group of non-repeating natural numbers.

6.2. Initialization

In the initialization step, two tasks will be performed, i.e. setting basic parameters of ACO and generating the solution space. The basic parameters mainly include the colony population, pheromone initial value and coefficients of key formulas in ACO. Literature (Wang et al., 2018) is used to generate the solution space.

6.3. Machining scheme generation

Generating a machining scheme includes two procedures, i.e. constituting workingsteps and selecting a workingstep sequence. In this study, a pheromone matrix (Fig. 4 (a)) and a pheromone vector (Fig. 4 (b)) are used to generate the workingstep sequence and workingsteps, respectively.

Fig. 5 gives the process of machining scheme generation. An ant first selects a workingstep according to the pheromone matrix, and then the ant will enter into the space of workingstep, where the workingstep is generated. After that, the ant leaves this space and starts to select the next workingstep. The above process will continue until all workingsteps are selected.

According to Fig. 4 (a), the pheromone matrix is important to select a workingstep. In the matrix, using the value located by WS_i and WS_j as the accordance to determine the next workingstep. The determination of the next WS (i.e. WS_j) is achieved based on the current WS (i.e. WS_i) except the first selection. Both i and j can represent the ID of a workingstep. For WS_i, when the selection starts, the i is fixed in general, and j is variable. Therefore, replacing i with constant c, and then the selection possibility of WS_j from WS_c, i.e. $P(c,j)$, can be completed by Eq. (25).

$$P(c,j) = \frac{\tau_{e\_c}^{\alpha}(j)\cdot(1/Ob(c,j))^{\beta}}{\sum_{j=0}^{n}\tau_{e\_c}^{\alpha}(j)\cdot(1/Ob(c,j))^{\beta}}, j \in allowed_{ws} \tag{25}$$

where $\tau_{e\_c}(j)$ is the pheromone vector extracted from the pheromone matrix when i is c (and it stores the pheromone value between workingstep c and the rest of the workingsteps), $Ob(c,j)$ is the evaluated value between workingstep c and workingstep j, $allowed_{ws}$ is the workingstep that is allowed to select, and α and β are the coefficients.

$$\begin{array}{c}
\begin{array}{cccccccccc}
 & WS_1 & WS_2 & WS_3 & WS_4 & WS_5 & WS_6 & WS_i & \cdots & WS_{n-1} & WS_n
\end{array}\\
\begin{array}{c} WS_1\\ WS_2\\ WS_3\\ WS_4\\ WS_5\\ WS_6\\ \vdots\\ WS_j\\ WS_{n-1}\\ WS_n \end{array}
\left[\begin{array}{ccccccccc}
0 & 0.65 & 0.89 & 0.67 & 0.27 & 0.53 & 0.81 & 0.61 & 0.52\\
0.56 & 0 & 0.91 & 0.72 & 0.61 & 0.47 & 0.75 & 0.78 & 0.65\\
0.98 & 0.47 & 0 & 0.81 & 0.49 & 0.34 & 0.62 & 0.83 & 0.44\\
0.32 & 0.82 & 0.11 & 0 & 0.91 & 0.63 & 0.45 & 0.13 & 0.35\\
0.65 & 0.12 & 0.37 & 0.31 & 0 & 0.21 & 0.55 & 0.52 & 0.87\\
0.25 & 0.28 & 0.78 & 0.41 & 0.61 & 0 & 0.75 & 0.66 & 0.72\\
 & & & \cdots\cdots & & & & \cdots\cdots & \\
0.74 & 0.81 & 0.71 & 0.26 & 0.82 & 0.56 & 0.77 & 0.82 & 0.65\\
0.36 & 0.82 & 0.34 & 0.61 & 0.63 & 0.64 & 0.45 & 0 & 0.11\\
0.35 & 0.35 & 0.61 & 0.37 & 0.74 & 0.12 & 0.22 & 0.37 & 0
\end{array}\right]
\end{array}$$

(a)

$$\begin{array}{ccc}
MT & & \tau_{MT}\\
0 & & 0.23\\
1 & & 0.11\\
2 & & 0.48\\
3 & & 0.35\\
4 & \longrightarrow & 0.43\\
5 & & 0.81\\
6 & & 0.78\\
\vdots & & \vdots\\
N_{MT} & & 0.47
\end{array}$$

(b)

Fig. 4. Pheromone matrix and vector.

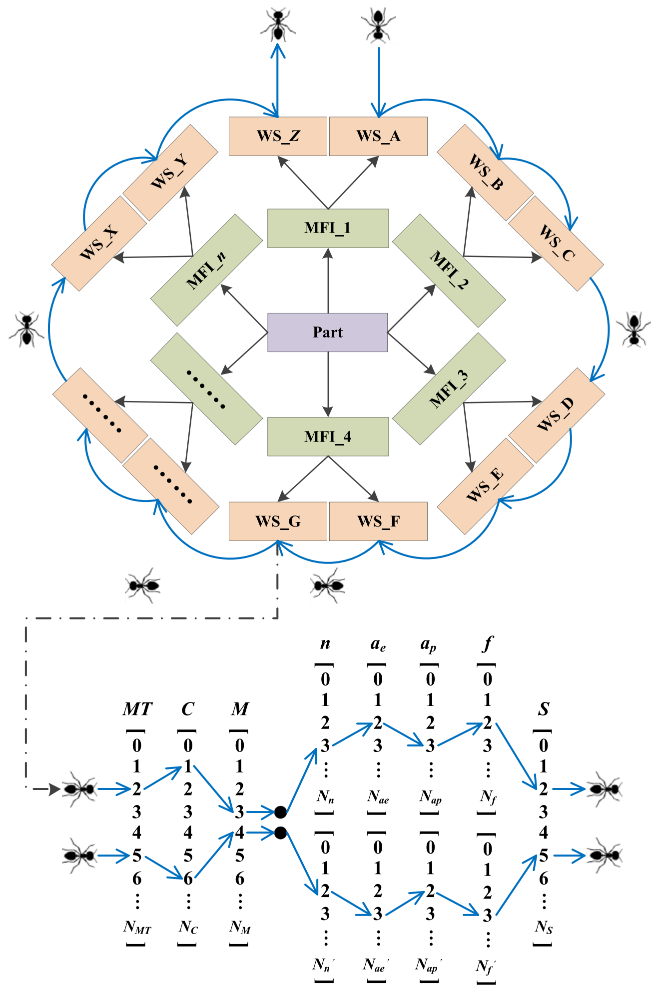

Fig. 5. Machining scheme generation.

Based on Eq. (25), Eq. (26) is given to achieve the selection of the next *WS*.

$$Num_{WS} = k, r_1 \le \sum_{j=0}^{k} P(c,j) \tag{26}$$

where Num_{WS} represents the ID of *WS*, r_1 is a random number that ranges from 0 to 1, and k is an ID of *WS*.

Eq. (26) represents the following process: calculating the sum of $P(c,j)$ with j ranging from 0 to n, and once the $P(c,k)$ is added to the previous sum, the kth *WS* is selected.

After the ID of a *WS* is selected, the elements of *WS* will be determined subsequently.

Regarding a *WS*, its elements include manufacturing resources, machining parameters and machining strategy. Each element has its own pheromone vector, for instance, Fig. 4(b) shows the pheromone vector of the machine tool. In terms of the pheromone vector, the possibility of an element of a *WS*, i.e. $P(i)$, is expressed by Eq. (27).

$$P(i) = \frac{\tau_e(i)}{\sum_{i=0}^{n}\tau_e(i)} \tag{27}$$

where τ_e represents the pheromone vector, i is the ID of an element, and n is the length of the pheromone vector.

Then, Eq. (28) is given to determine which ID of an element will be selected.

$$Ele_s = k, r_4 \le \sum_{i=0}^{k} P(i) \tag{28}$$

where r_4 is a random number that ranges from 0 to 1, k and i is the ID of the element of a *WS*.

Eq. (28) has the same meaning of Eq. (26), namely, calculating the sum of $P(i)$ with i from 0 to k; once the sum is greater than r_4, the k is selected.

To achieve optimization globally, the ants should have the chance to select the ID of workingstep and ID of an element of a *WS* randomly. Therefore, Eq. (29) and Eq. (31) are used to this purpose.

$$Num_{WS} = \begin{cases} Eq.(17), if\ r_2 \le Q \\ select\ randomly,\ else \end{cases} \tag{29}$$

$$Ele_s = \begin{cases} Eq.(19), if\ r_3 \le Q' \\ select\ randomly,\ else \end{cases} \tag{30}$$

6.4. Evaluation

In section 4.3, a machining scheme is generated. Next, this machining scheme should be evaluated. For the evaluation, the energy consumption model is used to calculate the energy efficiency of machining a part. Moreover, in each iteration, the evaluation of the current machining scheme will be compared with that of the previous machining scheme, and the better one will be used to achieve pheromone update.

6.5. Pheromone evaporation and update

During the iteration process, the pheromone will finish evaporation and update. Eq. (31) can be used to express the evaporation.

$$\tau_e \leftarrow (1-\gamma) \times \tau_e \tag{31}$$

where γ is the coefficient that ranges from 0 to 1.

Eq. (31) shows that the density of pheromone will decrease gradually. Meanwhile, the update will increase the density with the best generated machining scheme in one iteration. This process refers to Eq. (32).

$$\tau_e \leftarrow \tau_e + \frac{1}{SEC} \tag{32}$$

6.6. Tabu table

The tabu table covers the following functions:

- It meets the constraints, especially the constraints of the workingstep sequence.
- It meets the condition set by users.
- It stores the selected workingstep and workingstep sequence to avoid repetitive selection.

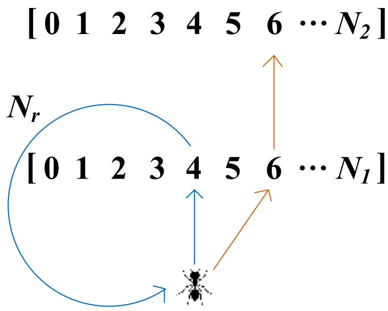

Fig. 6. Local multiple iteration.

Table 1
Machine tool information.

MT	Type	Machining capability			
		Roughness	Dimension error	Flatness tolerance	Position tolerance
ACE-50	Milling machine	3.2–6.3	±0.01	0.05	0.05
DMU-70		1.6–3.2	±0.005	0.01	0.01

Table 2
Cutting tool information.

CT	Type	Material	Diameter	CT	Type	Material	Diameter
CT1	EndMill	HSS	8	CT9	FaceMill	Carbide	63
CT2			9	CT10			80
CT3			10	CT11	T-slot	HSS	30
CT4			18	CT12			32
CT5		Carbide	10	CT13	Drill	HSS	8
CT6			18	CT14			10
CT7	FaceMill	HSS	10	CT15		Carbide	10
CT8		Carbide	50	CT16		HSS	15

6.7. An improved ACO

From the traditional ACO described above, there are some shortcomings: when determining a workingstep, there exist different dimensions of contributing factors to energy consumption, so that the lower dimension will result in earlier convergence and the higher dimension will do the opposite. This condition leads to the cost of the final iteration count. To overcome the drawbacks, this paper improves ACO with an approach called local multiple iteration.

As shown in Fig. 6, the improvement approach can be described as follows: in one iteration, an ant will repeat its action in the higher dimension of factors, leading to generation of more than one machining scheme. Then, these machining schemes are evaluated to select the best one to achieve the pheromone update. During this process, the following two principles can be referred to:

- The type of factor that is iterated multiply should not be too much, as otherwise the performance may deteriorate;
- This approach is to decrease the dimension difference of factors, so the time of the higher factor and lower one can be used as the iterated count.

7. Case study and discussions

This section will verify the presented approach using a case study. Firstly, power data acquirement experiment is performed to obtain the key coefficients of calculating energy consumption during machining operations. Then, the effectiveness of the improved ACO algorithm is verified by determining an energy-efficient machining scheme for a typical part. The performance of the traditional one and the improved one will be compared. Finally, the accuracy of energy consumption calculation method is given to indicate the effectiveness of the determined machining scheme.

7.1. Power data acquirement experiment

Two machine tools and sixteen cutting tools are selected as the experiment objects (the related information refers to Table 1 and Table 2). The material to be machined is C45 steel. The power meter is CW240. Fig. 7 shows the experimental platform used in this case study.

Table 3, Table 4 and Table 5 present the power of BC and MTFC,

Table 3
Power of BC and MTFC.

MT	BC (Unit: W)	WRC (Unit: W)			WURC (Unit: J)
		Light	Cutting Fluid	Chip removal	Tool changer
ACE-50	800	40	143	None	249
DMU-70	1740	60	162	235	615.5

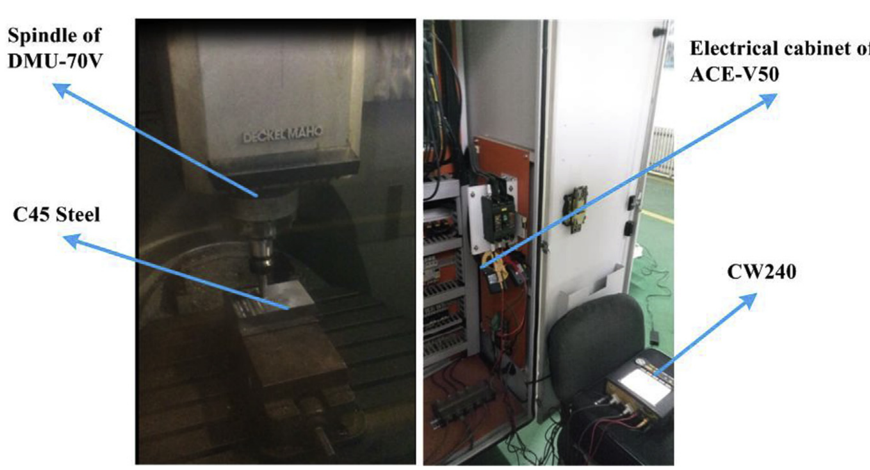

Fig. 7. Experiment scene.

Table 4
Power coefficient of spindle and feed axis.

MT	Sp		x FA		y FA		z FA			
	k	b	k_{1_x}	b_{1_x}	k_{1_y}	b_{1_y}	k_{1_z+}	b_{1_z+}	k_{1_z+}	b_{1_z-}
ACE-50	0.124	414.9	0.027	1.4	0.028	1.2	0.121	10.2	−0.013	−5.3
DMU-70	0.337	3.3	0.031	1.9	0.029	1.8	0.182	20.3	−0.022	−9.6

Table 5
Cutting power coefficient.

M	CT	MT	Coefficient				
			C_M	x	y	n	u
45# Steel	CT2	ACE-50	2.991	0.911	0.744	0.857	0.925
	CT4		2.832	0.926	0.731	0.821	0.900
	CT6		3.162	0.899	0.727	0.907	0.946
	CT8		5.889	0.883	0.710	0.889	0.921
	CT10		7.552	0.864	0.724	0.921	0.907
	CT14		32.323	–	0.843	0.973	–
	CT16		31.562	–	0.825	0.933	–
	CT3	DMU-70	3.659	0.985	0.706	0.917	0.937
	CT5		3.963	1.001	0.697	0.965	0.979
	CT7		4.668	1.001	0.710	0.976	0.959
	CT9		7.668	0.908	0.720	0.955	0.939
	CT12		5.964	1.039	0.746	1.006	1.001
	CT15		40.871	–	0.794	0.963	–

power coefficient of spindle and feed axis and cutting power coefficient, respectively. The detailed procedures can be found in the literature (Wang et al., 2018).

7.2. Verification

The part shown in Fig. 8 is used to verify the proposed model with the improved ACO solution. The solution space of ACO is obtained using the approach from (Wang et al., 2018), as shown in Table 6, Table 7 and Table 8.

Use Java programming language to implement the TACO and IACO, and then execute the two algorithms under the generated solution space before. The iteration process of TACO and IACO refers to Fig. 9: the two algorithms can converge when SEC is about 4.0 J/mm^3, and this shows that both of them can achieve the optimization. Besides, IACO needs less iteration counts to achieve convergence than TACO because of the introduce of local multiple iteration. But for IACO, the content of each iteration has been improved compared with TACO, so that each iteration time of the former may also increase. Thus, only checking iteration count is not enough to verify the effectiveness of IACO, and it is necessary to compare the time of two algorithms.

Fig. 10 gives the profile of each iteration time for IACO and TACO, and it shows that IACO will cost more time than TACO in each iteration. Referring to the data in Figs. 9 and 10, the convergence time of the two algorithms is shown in Table 9.

From the above table, the time for executing IACO is less than the time spent on executing TACO, and the efficiency is improved by approximately 25%. Regarding the time efficiency, IACO outperforms TACO in this case.

The generated machining scheme refers to Table 10, Table 11 and Table 12. It is necessary to obtain the error of calculated energy consumption and actual energy consumption.

Fig. 11 shows the machined part. Through power meter CW240, the actual energy consumption of machining the part is obtained. Therefore, the energy consumption model error can be calculated, which refers to Table 13.

According to Table 13, the error is approximately 7.22%. The result indicates that the proposed energy consumption model is able to calculate the required energy of a part. The next is to verify the quality, which includes geometric tolerancing and roughness. The checking process is shown in Fig. 12 and Fig. 13, and the result can be found in Table 14.

Table 14 displays the required value (RV) [um] and the measured value (MV) [um] of machining quality, and it implies that the part quality can meet the given requirements.

7.3. Discussion

The generated MS is further analysed and discussed, covering the workingstep and sequence of workingstep.

Table 10 gives the generated workingstep for milling, including the machine tool, cutting tool, strategy and parameters.

- In this table, except for WS_{p1_f2}, all workingsteps are implemented in ACE-V50, and WS_{p1_f2} is finished in DMU-70V. The result implies that ACE-V50 requires less energy consumption compared with DMU-70V during machining. But the requirement of WS_{p1_f2} is very stringent, and ACE-V50 cannot meet this. Hence, DMU-70V is selected to achieve the workingstep even though its energy demand is high.
- Regarding the cutting tool, the larger the diameter is, the higher its probability of selection will be. A cutting tool with large diameter will increase the range of parameters. Accordingly, a bigger material removal rate is easy to obtain, which will reduce the machining energy consumption.
- For strategies, CP is often selected during machining of a planar face or pocket. This is because this strategy produces less air cutting feed motion compared with other strategies.
- For parameters include f_z, v_M, a_w and a_p, according to Table 10, the values of f_z, a_w and a_p are near the maximum, but the value of v_M is intermediate. Regarding to v_M, its value is limited by tool life.

Table 12 gives the generated workingstep sequence and it can be found that the workingstep is sequenced on the basis of the least time of changing cutting tools to reduce the energy demand of the preparation state. This sequence limits the machine of planar face artificially, where $WS_{p1_r}$is first and followed by WS_{p1_f1}. The purpose is to provide a preliminary plane for manufacturing subsequent features. In addition, the location of WS_{p1_f2} is not limited, and the improved ACO selects the workingstep as the last one. The reasons are: WS_{p1_f2} needs another machine tool to implement, leading to the operation of changing machine tool. If WS_{p1_f2} is executed before other workingstep, this sequence will produce two operations of changing machining tool. Therefore, WS_{p1_f2} is the final workingstep.

Moreover, compared with (Wang et al., 2018), this paper achieves the following improvement:

- The energy consumption model considers a holistic process of the working piece.

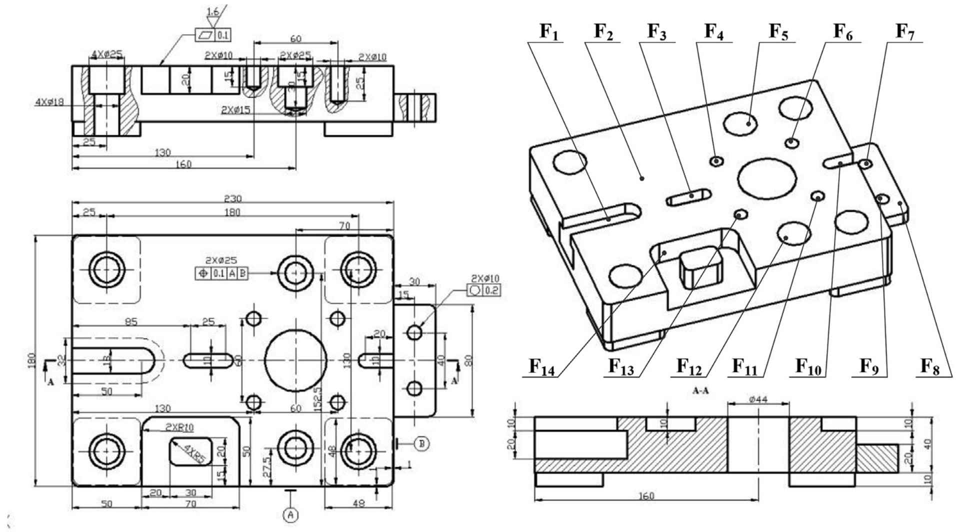

Fig. 8. Test part of verifying improved ACO.

Table 6
Solution space (part 1 - machining resource, operation and strategy).

NO.	N_MF	MF	S	Op	Tool	MT
1	F1	T-Slot	CM	BSRM(Up)	CT6	ACE-V50,
2					CT4	DMU-70V
3				BSRM(Down)	CT12	
4	F2	Planar face	BD UD CP	PRM	CT8	
5					CT9	
6					CT10	
7			BD UD CP	PSFM	CT8	
8					CT9	
9					CT10	
10			BD UD CP	PFM	CT10	DMU-70V
11	F3	Slot	CM	BSRM	CT3	ACE-V50,
12					CT5	DMU-70V
13	F10	Slot	CM	BSRM	CT3	
14					CT5	
15	F8	Step	BD UD CP	BSRM	Endmills in Table 2	
16	F14	Pocket	BD_C C_BD	BSRM		
17	F4, F9, F6,	Round hole	DR	DO	CT14	
18	F7, F13, F11				CT15	
19	F5, F12	Compound feature	CP	BSRM(Up)	CT2	
20					CT3	
21					CT5	
22			DR	DO (Down)	CT16	
23	Datum A, Datum B	Datum	BD UD CP	PSFM SSFM	Endmills or facemills in Table 2	

Table 7
Solution space (part 2 - parameter range of milling).

Num	max_fz	min_fz	max_aw	min_aw	max_ap	min_ap	max_v	min_v
1	0.150	0.002	18	2	9	0.2	180	50
3	0.035	0.002	32	32	10	10	80	30
5	0.160	0.002	63	5	30	2	500	120
7	0.120	0.002	50	5	25	2	450	100
9	0.120	0.004	80	10	35	5	650	150
11	0.070	0.004	10	0.5	4	0.1	110	45
13	0.070	0.004	10	0.5	6	0.1	110	45
19	0.065	0.003	3.5	0.1	9	0.5	105	55
21	0.075	0.005	5	0.1	10	0.5	120	65

Table 8
Solution space (part 3 - parameter range of drilling).

Num	max_fr	min_fr	max_v	min_v
17	0.3	0.15	110	60
18	0.28	0.12	105	58
22	0.32	0.18	120	70

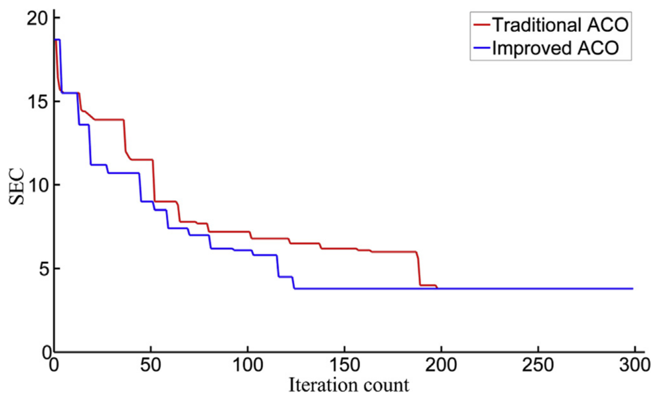

Fig. 9. Iteration process of TACO and IACO.

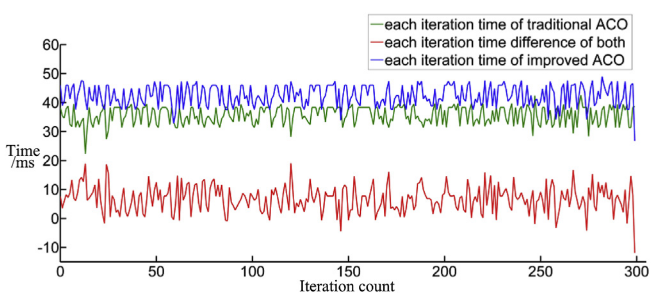

Fig. 10. Time of each iteration.

Table 9
Time of executing and TACO (Unit: ms).

Time of executing IACO	Time of executing TACO
5286.94	7082.49

Table 10
Generated workingstep for milling.

MF	WS	S	MT	T	P			
					f_z	v_M	a_w	a_p
F_1	WS_{ts1_r1}	CM	ACE-V50	CT4	0.115	56.9	18	8.1
	WS_{ts1_r2}			CT12	0.032	45.7	32	10
F_2	WS_{p1_r}	CP		CT10	0.150	102.4	50	15
	WS_{p1_f1}			CT10	0.110	132.4	50	4
	WS_{p1_f2}		DMU-70V	CT10	0.080	173.1	35	1
F_3	WS_{s1_r}	CM	ACE-V50	CT3	0.069	61.9	10	5.7
F_8	WS_{step1_r}	CP		CT6	0.101	62.4	18	8.5
F_{10}	WS_{s2_r}	CM		CT3	0.070	62.2	10	5.4
F_{14}	$WS_{pocket1\_r}$	CP		CT6	0.069	69.6	20	3.8
F_5	WS_{h2_r2}			CT3	0.074	75.1	4.3	9.2
F_{12}	WS_{h7_r2}			CT3	0.073	73.1	4.6	9.7
Datum A	WS_{datumA}	CP	ACE-V50	CT6	0.105	86.7	3	15.8
Datum B	WS_{datumB}	CP	ACE-V50	CT6	0.103	87.4	3	15.6

Table 11
Generated workingstep for drilling.

MF	WS	S	MT	T	P	
					f_r	v_D
F_4	WS_{h1_r}	CM	ACE-V50	CT14	0.286	74.24
F_5	WS_{h2_r1}	DR		CT16	0.318	73.11
F_6	WS_{h3_r}			CT14	0.279	75.28
F_7	WS_{h4_r}			CT14	0.281	75.02
F_9	WS_{h5_r}			CT14	0.271	76.32
F_{11}	WS_{h6_r}			CT14	0.275	75.91
F_{12}	WS_{h7_r1}			CT16	0.311	73.80
F_{13}	WS_{h8_r}			CT14	0.29	73.61

Table 12
Generated workingstep sequence.

Workingstep sequence
WS_{p1_r} -> WS_{p1_f1} -> WS_{datumA} -> WS_{datumB} -> WS_{h9_r} -> WS_{h1_r} -> WS_{h3_r} -> WS_{h6_r} -> WS_{h5_r} -> WS_{h4_r} -> WS_{h7_r1} -> WS_{h2_r1} -> WS_{h7_r2} -> WS_{h2_r2} -> WS_{s1_r} -> WS_{s2_r} ->WS_{ts1_r1} -> WS_{ts1_r2} -> $WS_{pocket1\_r}$ -> WS_{step1_r} -> WS_{p1_f2}

Fig. 11. Test part that has been machined.

Table 13
Energy consumption model error.

CEC(KJ)	MEC(KJ)	Error
4712.21	4372.10	7.22%

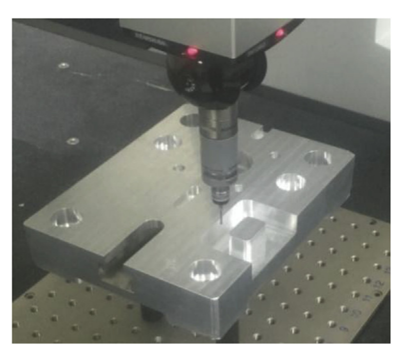

Fig. 12. Checking position tolerancing.

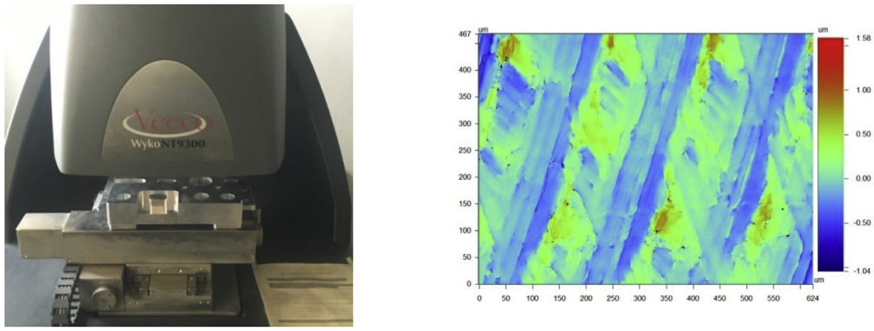

(a) Wyko NT930 (b) result of roughness

Fig. 13. Checking roughness.

Table 14
Result of checking quality.

Roughness		Flatness		Position		Circularity	
RV	MV	RV	MV	RV	MV	RV	MV
1.6	1.11	0.1	0.81	0.1	0.92	0.2	0.17

- Based on the established energy consumption model, ACO is employed to generate BMS for a complete part, and its performance is enhanced by local multiple iteration.

8. Conclusions

This paper presents an optimization model considering energy-efficient machining for prismatic parts via STEP-NC and its solution with an improved ACO algorithm. Workingstep in STEP-NC is adopted to achieve the calculation of energy consumption. Accordingly, the optimization model is then built with the optimization objective, optimization variable and constraints. An improved ACO algorithm is applied to solve the proposed model. The proposed optimized approach is verified by a part with typical manufacturing features. The result shows that:

- The calculation method of energy consumption is effective to calculate the energy demand of the machining of an entire part.
- The optimized solution can provide a comprehensive machining scheme for low energy demand, which meets the given requirements simultaneously.
- The ideal of local multiple iteration in ACO can improve the efficiency of solving the optimization problem.

The main advantages of this work can be summarized as follows: The use of STEP-NC makes the energy consumption calculation obtain the machining energy of a whole part from a holistic perspective. Followed by the energy calculation approach, the optimization model could optimize energy consumption by adjusting machining resources, parameters, strategies, operations, etc. For the above reviewed energy optimization method, only one or portions of contributing factors to energy consumption (e.g., parameters) are considered. The proposed method of this paper could overcome this drawback.

This work aims at prismatic parts with 2.5D manufacturing features to present the energy optimization approach. But there are increasingly more products with complex surfaces in the market, where the energy consumption characteristics is also a challenge. Therefore, the energy consumption model of complex surfaces and its optimization method will be performed in our future work. In addition, this paper mainly focuses on production phase of sustainable product lifecycle management to implement energy-efficient machining based on STEP-NC. The proposed framework can be extended to the whole process of sustainable product lifecycle management. And this is also the next research point in the future.

Acknowledgements

This work has been supported by the National Natural Science Foundation of China (Grant No. 51175485).

Nomenclature

E_{part}	energy consumption of machining a part [J]
$E_{ws,i}$	ith workingstep energy [J]
E_p	energy demand of the preparation state [J]
E_a	energy demand of the approaching state [J]
E_l	energy demand of the leaving state [J]
E_m	energy demand of the machining state [J]
E_{b,ws_nr}	energy consumption of BC and WURC [J]
E_{m_r}	energy consumption of rapid traverse in the machining state [J]
E_{m_f}	feed axis energy consumption in the machining state [J]
E_{m_c}	cutting energy consumption in the machining state [J]
t_{total}	total time of machining a part [s]
$t_{p,i}$	preparation state time of the ith workingstep [s]
$t_{l,i}$	leaving state time of the ith workingstep [s]
$t_{a,i}$	approaching state time of the ith workingstep [s]
$t_{m,i}$	machining state time of the ith workingstep [s]
t_l	leaving state time of a workingstep [s]
t_a	approaching state time of a workingstep [s]
t_m	machining state time of a workingstep [s]
$P_{ws,nr}$	power of WURC [W]
P_b	power of BC [W]
$P_{a,l}$	power of the feed axis in the approaching state or leaving state [W]
P_{m_c}	cutting power [W]
P_{m_f}	feed axis power [W]
P_M	milling power [W]
P_D	drilling power [W]
v_r	velocity of rapid traverse [mm/min]
f_r	feed per revolution [mm/r]
v_M	cutting velocity for milling [m/min]
v_D	cutting velocity for drilling [m/min]
a_p	axial cutting depth [mm]
f_z	feed per tooth [mm/z]
a_w	radial cutting depth [mm]
T	tool life [h]

T_l expected tool life [h]

References

Altıntaş, R.S., Kahya, M., Ünver, H.Ö., 2016. Modelling and optimization of energy consumption for feature based milling. Int. J. Adv. Manuf. Technol. 86 (9–12), 1–19.

Aramcharoen, A., Mativenga, P.T., 2014. Critical factors in energy demand modelling for CNC milling and impact of toolpath strategy. J. Clean. Prod. 78, 63–74.

Avram, O.I., Xirouchakis, P., 2011. Evaluating the use phase energy requirements of a machine tool system. J. Clean. Prod. 19 (6–7), 699–711.

Borgia, S., Albertelli, P., Bianchi, G., 2017. A simulation approach for predicting energy use during general milling operations. Int. J. Adv. Manuf. Technol. 90 (9), 3187–3201.

Camposeco-Negrete, C., 2013. Optimization of cutting parameters for minimizing energy consumption in turning of AISI 6061 T6 using Taguchi methodology and ANOVA. J. Clean. Prod. 53 (16), 195–203.

Chen, X., Tang, Y., Li, C., Yi, Q., 2015. Multi-objective parameter optimization of multi-pass CNC machining. In: IEEE International Conference on Automation Science and Engineering, pp. 45–50.

Deng, Z., Zhang, H., Fu, Y., Wan, L., Liu, W., 2017. Optimization of process parameters for minimum energy consumption based on cutting specific energy consumption. J. Clean. Prod. 166, 1407–1414.

Gong, X., De Pessemier, T., Joseph, W., Martens, L., 2016. A generic method for energy-efficient and energy-cost-effective production at the unit process level. J. Clean. Prod. 113, 508–522.

He, Y., Li, Y.F., Wu, T., Sutherland, J.W., 2015. An energy-responsive optimization method for machine tool selection and operation sequence in flexible machining job shops. J. Clean. Prod. 87, 245–254.

ISO14649-1, 2003. Industrial Automation Systems and Integration-Physical Device Control-Data Model for Computerized Numerical Controllers-Part 1:overview and Fundamental Principles. International Organization for Standardization, Geneva, Switzerland.

Jia, S., Tang, R.Z., Lv, J.X., 2014. Therblig-based energy demand modeling methodology of machining process to support intelligent manufacturing. J. Intell. Manuf. 25 (5), 913–931.

Jia, S., Tang, R.Z., Lv, J.X., 2016. Machining activity extraction and energy attributes inheritance method to support intelligent energy estimation of machining process. J. Intell. Manuf. 27 (3), 595–616.

Kara, S., Li, W., 2011. Unit process energy consumption models for material removal processes. CIRP Ann. - Manuf. Technol. 60 (1), 37–40.

Li, C., Li, L., Tang, Y., Zhu, Y., Li, L., 2019. A comprehensive approach to parameters optimization of energy-aware CNC milling. J. Intell. Manuf. 30 (1), 123–138.

Li, J.G., Lu, Y., Zhao, H., Li, P., Yao, Y.X., 2014. Optimization of cutting parameters for energy saving. Int. J. Adv. Manuf. Technol. 70 (1), 117–124.

Liu, N., Zhang, Y.F., Lu, W.F., 2015. A hybrid approach to energy consumption modelling based on cutting power: a milling case. J. Clean. Prod. 104, 264–272.

Lv, J.X., Tang, R.Z., Jia, S., Liu, Y., 2016. Experimental study on energy consumption of computer numerical control machine tools. J. Clean. Prod. 112, 3864–3874.

Lv, J., Tang, R., Tang, W., Jia, S., Liu, Y., Cao, Y., 2018. An investigation into methods for predicting material removal energy consumption in turning. J. Clean. Prod. 193, 128–139.

Ma, F., Zhang, H., Cao, H., Hon, K.K.B., 2017. An energy consumption optimization strategy for CNC milling. Int. J. Adv. Manuf. Technol. 90 (5), 1715–1726.

Peng, T., Xu, X., 2017. An interoperable energy consumption analysis system for CNC machining. J. Clean. Prod. 140, 1828–1841.

Shi, K.N., Zhang, D.H., Liu, N., Wang, S.B., Ren, J.X., Wang, S.L., 2018. A novel energy consumption model for milling process considering tool wear progression. J. Clean. Prod. 184, 152–159.

Shrouf, F., Ordieres-Mere, J., Garcia-Sanchez, A., Ortega-Mier, M., 2014. Optimizing the production scheduling of a single machine to minimize total energy consumption costs. J. Clean. Prod. 67 (6), 197–207.

Tan, X.C., Liu, F., Cao, H.J., 2004. Decision-making model for process route in green manufacturing and its algorithms. J. Mech. Eng. 40 (4), 154–159.

Velchev, S., Kolev, I., Ivanov, K., Gechevski, S., 2014. Empirical models for specific energy consumption and optimization of cutting parameters for minimizing energy consumption during turning. J. Clean. Prod. 80, 139–149.

Wang, H., Xu, X., Zhang, C., Hu, T., 2018. A hybrid approach to energy-efficient machining for milled components via STEP-NC. Int. J. Comput. Integr. Manuf. 31 (4–5), 442–456.

Wang, Q., Liu, F., Wang, X., 2014. Multi-objective optimization of machining parameters considering energy consumption. Int. J. Adv. Manuf. Technol. 71 (5), 1133–1142.

Yan, J.H., Li, L., 2013. Multi-objective optimization of milling parameters – the trade-offs between energy, production rate and cutting quality. J. Clean. Prod. 52 (4), 462–471.

Yi, Q., Li, C.B., Tang, Y., Chen, X.Z., 2015. Multi-objective parameter optimization of CNC machining for low carbon manufacturing. J. Clean. Prod. 95, 256–264.

Yoon, H.-S., Singh, E., Min, S., 2018. Empirical power consumption model for rotational axes in machine tools. J. Clean. Prod. 196, 370–381.

Zhang, Z.W., Tang, R.Z., Peng, T., Tao, L.Y., Jia, S., 2016. A method for minimizing the energy consumption of machining system: integration of process planning and scheduling. J. Clean. Prod. 137, 1647–1662.

Zhong, Q., Tang, R., Lv, J., Jia, S., Jin, M., 2016. Evaluation on models of calculating energy consumption in metal cutting processes: a case of external turning process. Int. J. Adv. Manuf. Technol. 82 (9), 2087–2099.

Zhou, L.R., Li, J.F., Li, F.Y., Meng, Q., Li, J., Xu, X.S., 2016. Energy consumption model and energy efficiency of machine tools: a comprehensive literature review. J. Clean. Prod. 112, 3721–3734.